FPFD Radio Isotope Heat Sourced Stirling Engine for Powering Stirling Cooler and other Devices in Space

M. A. Krishnan, B. T. Kuzhiveli

Center for Advanced Studies in Cryogenics,
National Institute of Technology Calicut, India 673601

ABSTRACT

Cryocoolers are used in space applications to cool the sensors and other electronic equipment. In satellites, image capturing sensors are used for enhancing the spectral coverage range of these devices from visible to far-infrared, which requires low-temperature cooling. An onboard power system is used to drive the cryocooler. This poses significant challenges if traditional solar arrays are used to power the spacecraft.

Currently Radioisotope Thermoelectric Generator (RTG) are used. Dynamic Radioisotope Power systems, which are far more efficient compared to solar arrays are still under development and their capability to power the cryocooler along with other subsystems in the spacecraft has not been studied extensively. In this study, a Free Piston Stirling Engine (FPSE), in the medium power range, is designed to work with Radioisotope Power Source to power the spacecraft. Part of the generated power is used to run a Stirling cryocooler, which is designed to work with minimum power. Both the engine and the cryocooler are designed using SAGE software and the engine results are verified using an axisymmetric 2D CFD analysis in ANSYS Fluent©.

The designed engine is found to have a maximum efficiency of 40% at a power output of 250 W and is found to be sufficient to power the cryocooler as well as other subsystems in the spacecraft.

INTRODUCTION

Space exploration requires a power supply for the spacecraft to operate and solar power has significant limitations if it is used for this purpose. The intensity of sunlight is inversely proportional to the square of the distance from the sun and decreases significantly towards outer space. Radioisotope Power Systems can prove to be a suitable alternative in such cases. [1] Energy converters used in RPS are of two types: static and dynamic conversion systems. [2] Free piston Stirling engines are one of the most efficient dynamic conversion systems due to their advantages, such as long operating life without the need for lubrication, high efficiency, high reliability, and quiet easy operation. [3] The variations in the internal pressure of the FPSE drive its power piston, which is connected to the reciprocating magnets in a linear alternator (LA) for electricity production. [4] The coupled mechanical dynamics and thermodynamics in an FPSE make its design more complicated.

The preliminary stage of the design process involves using a one-dimensional thermodynamic modelling tool such as SAGE modelling software. [5] More accurate multidimensional CFD models have also been used in the past to design and optimize the engine. [6] The CFD analysis has many advantages such as its ability to model inherently multi-dimensional entities such as turbulent fluid flow patterns.

Cryocoolers 22, edited by R.G. Ross, Jr., J.R. Raab and S.D. Miller

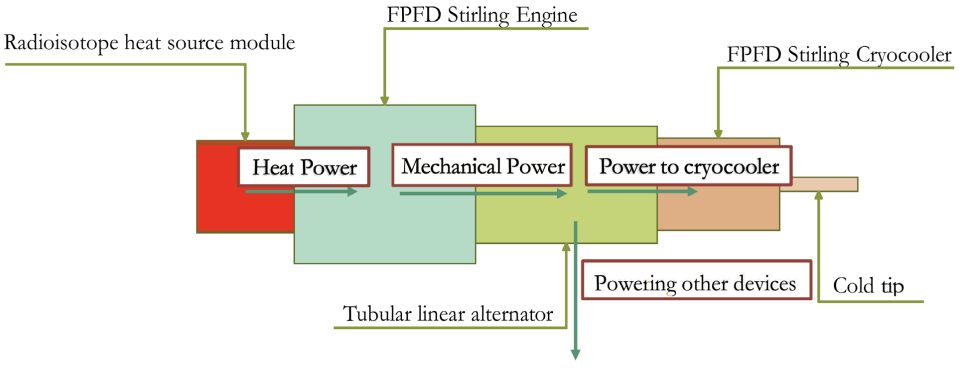

Figure 1. Concept of integrated system

This paper describes the design and integration of a free-piston Stirling engine-linear alternator power system with a free-piston Stirling cryocooler (Figure 1). Initially, a free piston Stirling engine is designed, optimizing the geometrical as well as operating parameters of the engine using SAGE software and verifying the performance using a computational fluid dynamics simulation of the designed engine using commercial software, ANSYS Fluent©. [7] The results from the SAGE software are compared to the CFD results and reported. Further, a Stirling split-type cryocooler is also designed for a 0.75 W at 80 K heat lift and minimum compressor power. This value of heat lift was found to be sufficient for many advanced cameras and other sensors used in space applications. The engine is optimized for a medium power output of 250 W and it is found to be sufficient for powering the cryocooler, which requires a power input of nearly 8 W, and many other devices in the spacecraft.

FREE PISTON STIRLING ENGINE DESIGN

Sage optimization

The SAGE Library contains many generic Stirling device components that can be placed and connected in the Graphical User Interface of SAGE. [8] Components and sub-components exist hierarchically to define the system or subsystem being modelled as shown in Figure 2.

For the process of modelling, a model of a free piston Stirling engine with displacer arranged coaxially within an annular heat rejector and regenerator assembly was used. The tubular type heater was used with several bent tubes. The work output of the engine was constrained to be 250 W and the

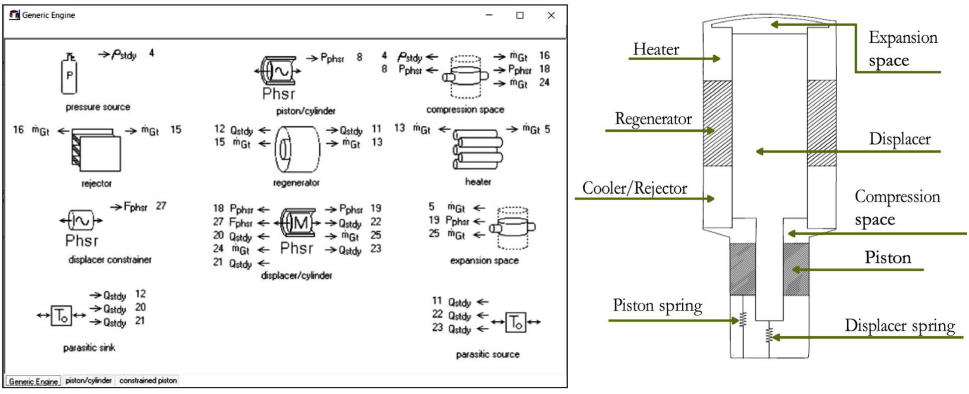

Figure 2. Sage user interface of FPSE (left) and FPSE illustration (right) [8]

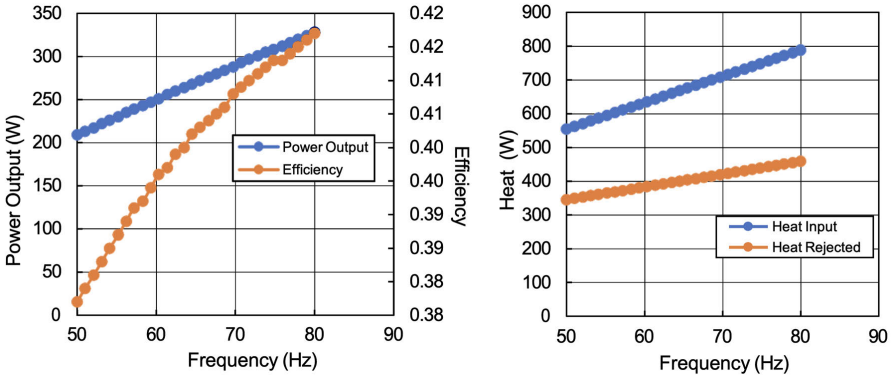

Figure 3. SAGE frequency mapping

objective of the optimization was to maximize the efficiency. Mapping was also performed to find out the change in performance parameters of the engine with a change in design variables (Figure 3).

CFD verification

For the CFD study, the Navier Stokes Equation using the SST k-ω turbulence model was used for the parameters used to measure the instantaneous pressure and viscous forces determined at discrete time and space points. [9,10] A pressure based solver with absolute velocity formulation was used. Two-dimensional axisymmetric transient simulation was conducted using helium as the working fluid. The properties of helium were obtained by FLUENT© from the real-gas-helium NIST data. The Fluent© PISO algorithm was used to solve the pressure velocity coupling and Fluent© PRESTO! routine was used for pressure interpolation. Structured quadrilateral mesh (Figure 4) with high quality was used, and was progressively refined near the walls to obtain the boundary layer mesh. The number of elements was nearly 25,000. Figure 5 shows the pressure contour and velocity vectors at different times during the transient simulation. Data from Table 1 was the input for the geometry and the final results of the simulation are reported in Table 2. The differences in power output, heat input and efficiency of the engine obtained using CFD and Sage software are found to be reasonably small. The engine is expected to produce a mechanical power output of 230.9 W at an efficiency of 30.52%. For producing the required heat of 756.52 W, the amount of radioisotope plutonium can be found from the following equation:

$$P = 1.6\times10^{-3}\,\frac{E\lambda A v}{M} \tag{1}$$

The specific power was obtained from the equation to be 0.56 W/gm. 1.35 kg of plutonium would be required to produce the required heat from the radioisotope at the beginning of mission. The amount of plutonium undergoes decay during the course of the mission and the amount available at the Year of Mission (YOM) is given by the equation:

$$\text{YOM Fuel load} = \text{BOM Fuel load} \times 0.5^{87.74} \tag{2}$$

Even after 18 years of mission, more than 650 W of fuel load will be available. If the engine operates at 30% efficiency, 195 W of mechanical power output would be produced, which even after considering the alternator efficiency, would be sufficient for devices in the spacecraft to operate.

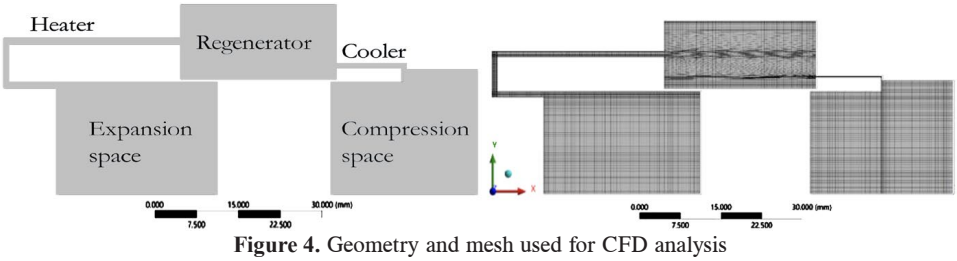

Figure 4. Geometry and mesh used for CFD analysis

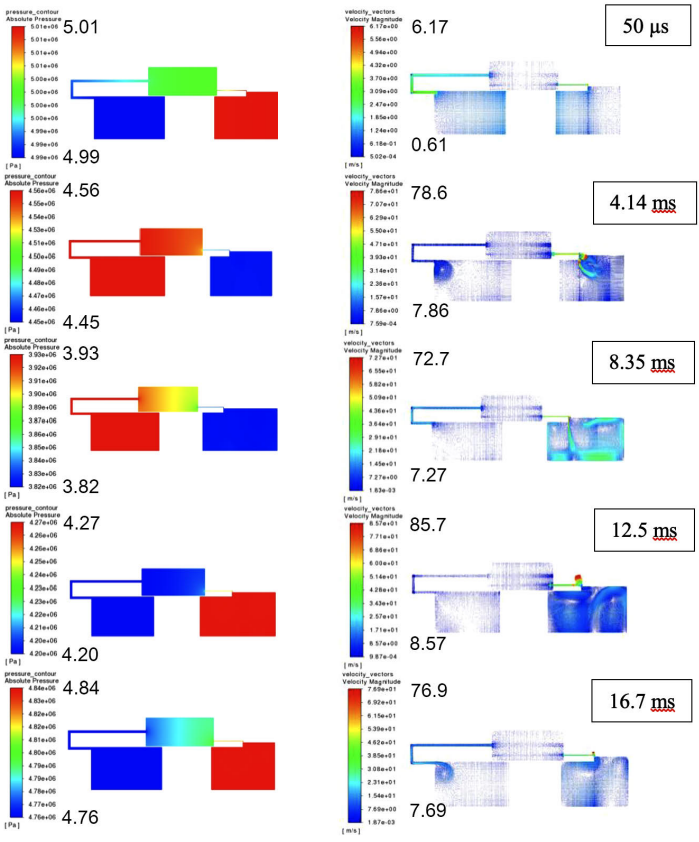

Figure 5. Pressure contours, Pa x 10^6 , (left) and velocity vectors, m/s, (right) at different instants of CFD simulation

Table 1. Parameters of Optimized engine

Parameter	Value	Parameter	Value
Working gas	Ideal Helium	Piston Amplitude	6 mm
Charge Pressure	5 MPa	Compression space length	2.63 cm
Frequency	60 Hz	Rejector Length	2 cm
Heat input	637.1 W	Regenerator Length	2.8 cm
Net Power Output	250 W	Regenerator Matrix ID	3.52 cm
Efficiency	39.24 %	Heater Length	4.61 cm
Regenerator Porosity	69.69 %	Displacer Length	3 cm
Displacer spring stiffness	6722 N/m	Displacer OD	3.9 cm
Pressure Wall ID	5.941 cm	Displacer Amplitude	3.25 mm
Piston OD	3.9 cm	Displacer drive rod diameter	2.32 mm

Table 2. Comparison of SAGE and CFD Results

	CFD Result	SAGE Result	Difference
Power Output	230.9 W	250 W	19.1 W
Efficiency	30.52%	39.24%	8.72 %
Heat Input	756.52 W	637.1 W	119.42 W

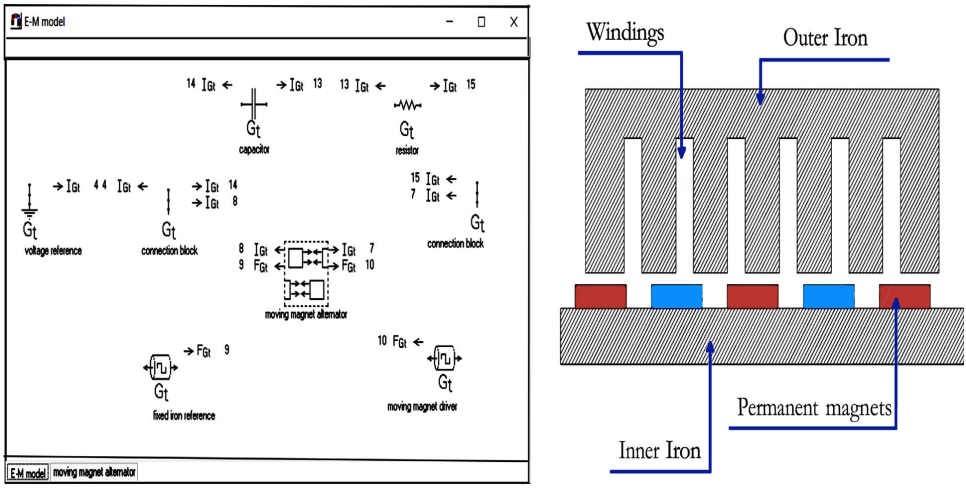

Figure 6. Sage user interface of PMLA (left) and PMLA illustration (right)

LINEAR ALTERNATOR DESIGN

Sage optimization

A tubular type single phase permanent magnet design has been chosen for the linear alternator. A single magnet and pole arrangement have been chosen to reduce the mass of the device and make it compact. SAGE models the moving magnet motor/alternator with a radially polarized permanent magnet moving back and forth within the gap between the inner and outer iron (Figure 6). The alternating magnetic flux in the inner iron results in flux linking with the coil windings and completes the magnetic circuit through the outer iron. The pieces of the pole and the space between for the copper coils are assumed to have the same length. The design point amplitude of the magnet is also taken to be half of this length. The model parameters are optimized using the Sage optimizer and the results are shown in Table 3.

ANSYS Maxwell analysis

A 2D axisymmetric model of the permanent magnet linear alternator (PMLA) [11] was created in ANSYS Maxwell. The magnetic transient solver was used for the Finite Element analysis.

Table 3. Optimized results of LA from Sage

Parameter	Value	Parameter	Value
Frequency	60 Hz	Inner iron radius	3.5 cm
Alternator efficiency	91.92 %	Magnetic gap	7.5 mm
Number of turns in the coil	623	Outer iron radius	4.25 cm
Coil I^2R loss	0.109 W	Coil Height	1.5 cm
Eddy current loss	1.4981 W	Inner iron thickness	8 mm
Hysteresis loss	0.4051 W	Outer iron inner thickness	6.588 mm
Reciprocating mass	1 kg	Outer iron outer thickness	4.87 mm
Load Resistance	89.96 Ohm	Wire diameter	0.8306 mm
Coil Packing factor	0.9	Poles separation	2.5 cm
Pole length	22.5 cm		

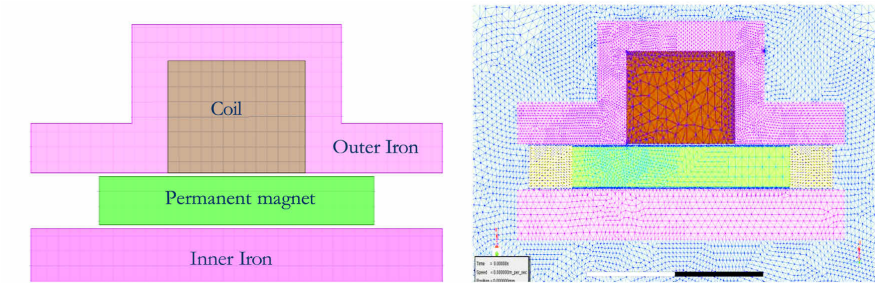

Figure 7. Asymmetric geometry (left) and mesh (right) of tubular linear alternator

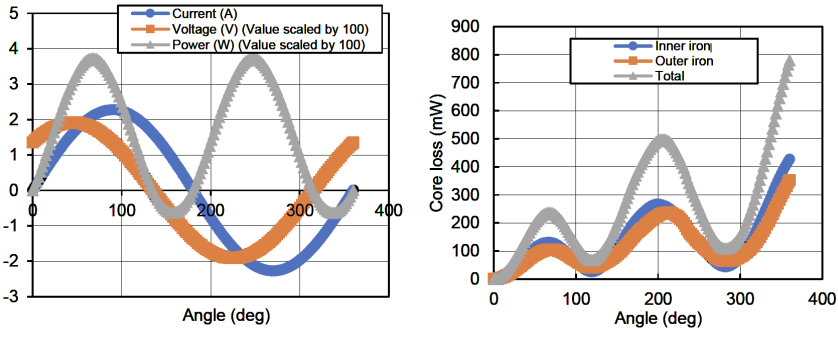

Figure 8. Results from Maxwell simulation

The permanent magnet was the source of the magnetic field and the core losses in the ferromagnetic core were modeled using an electrical/steel model. Mechanical transients were modeled with force and damping values to approximate the oscillatory motion of the power piston. The model of the magnetic circuit is shown in Figure 7 and results of the model are provided in Figure 8.

CRYOCOOLER DESIGN

SAGE optimization

The cryocooler is designed to operate with a cold end temperature of 80 K [12] and to have a heat lift of 750 mW. The function of the optimization is to minimize the work input while the constraint of 0.75 W is placed on the heat lift. The parameters of the designed cooler are given in Table 4. The performance parameters of the engine, i.e., heat lift, work input and COP of the system are mapped for a range of frequencies and charge pressures and plotted in Figure 9.

Table 4. Parameters of the designed Cryocooler

Parameters	**Values**	**Parameters**	**Values**
Heat Lift	0.75 W	Displacer diameter	5 mm
Heat Rejected	0.7903 W	Compression space 1 length	5 mm
Work input	7.256 W	Compression space 2 length	2.5 mm
Displacer spring stiffness	2003 N/m	Regenerator material	SS304
Displacer phase angle	51.81 deg	Regenerator porosity	0.69
Piston length	40 mm	Regenerator wire diameter	0.0254 mm
Piston diameter	6 mm	Regenerator wire mesh no	400
Piston amplitude	5.867 mm	Connecting tube length	10 mm
Displacer length	50 mm	Expansion space length	3 mm

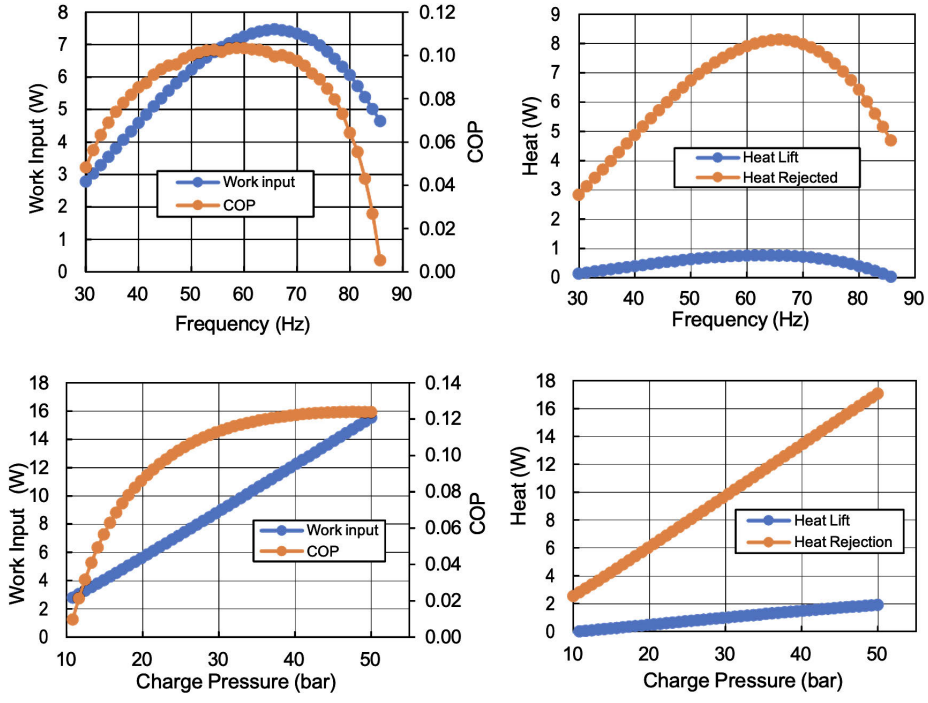

Figure 9. SAGE mapping of frequency and charge pressure of the cryocooler

FINAL INTEGRATED SYSTEM

The plutonium radioisotope delivers a heat input of 756 W at the beginning of mission to the FPFD Stirling engine, which converts it to a mechanical power output of 250 W in the form of oscillatory motion of the power piston. The linear alternator further converts the mechanical power output to electrical power. The FPSC requiring a power input of almost 7.3 W for producing a cooling of 750 mW, while maintaining the cold tip at 80 K, is integrated with the FPSE-alternator system (Figure 10). The rest of the power from the power system is used to power other devices in the spacecraft and keep the spacecraft warm in space. Although the heat input from the radioisotope deteriorates during the course of the mission, the power output even after 18 years, would still be close to 190 W. This is sufficient to keep the FPFD Stirling cooler and other devices working.

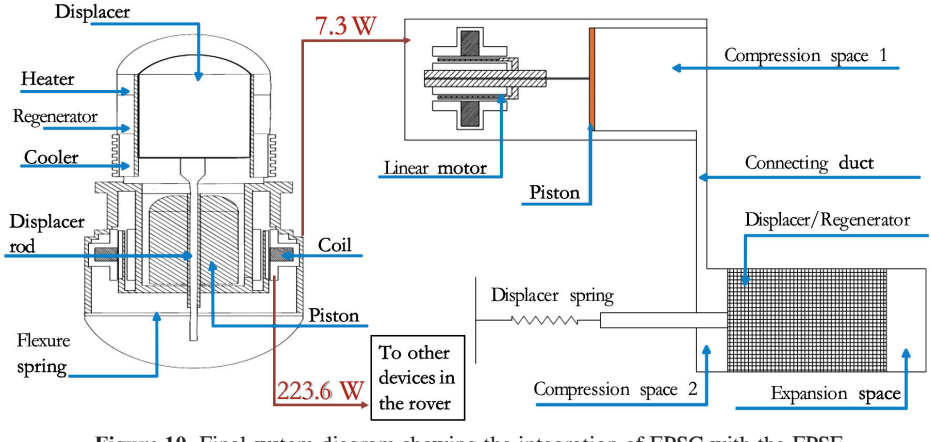

Figure 10. Final system diagram showing the integration of FPSC with the FPSE

Table 5. Comparison of the results of LA from Sage and ANSYS Maxwell

Parameters	ANSYS Maxwell	SAGE	Difference
Average Power Output (W)	217.35	223.1	5.75
Core Loss (W)	0.601	1.903	1.302

CONCLUSION

The beta-type FPSE has been designed using SAGE and ANSYS Fluent analysis and the amount of plutonium required for providing the required amount of heat to the engine is calculated using standard equations. The tubular-type permanent magnet linear alternator has been designed using Sage and ANSYS Maxwell analysis and integrated with the FPSE. Further, a split-type FPFD Stirling cooler has been designed using Sage. Finally, The FPFD Stirling engine-linear alternator power system has been integrated with the FPFD Stirling cryocooler. The power system has been found to be sufficient to power the cryocooler and other devices in the spacecraft. From previous research, most other devices would require less than 110 W combined. Therefore, the excess power can be stored in a battery and used during the period of peak power demand. Difference between SAGE and 2D CFD results for FPSE and the linear alternator are relatively small, except for the core losses. The results shown in Table 5 support the validity of SAGE code in accurately predicting model performance in much lesser time than other multidimensional models.

REFERENCES

1. N. R. C. of the National Academies, *Radioisotope Power Systems: An Imperative for Maintaining U.S. Leadership in Space Exploration Radioisotope*, The National Academies Press, (2009).
2. A. Mazzetti, M. Gianotti, G. Pinarello, L. Celotti, "Heat to electricity conversion systems for moon exploration scenarios : A review of space and ground technologies," *Acta Astronaut*, vol. 156, (2019), pp. 162–186.
3. G. Walker, J. R. Senft, *Free-Piston Stirling Engines,* Springer-Verlag, New York, (1985) pp. 22–99.
4. NASA, "Advanced Stirling Radioisotope Generator (ASRG)," *NASA Facts*, (2013), pp. 1–2.
5. J. F. Metscher, *Free-Piston Stirling Convertor Model Development, Validation, and Analysis for Space Power Systems*, Dissertations and Theses, Embry Riddle Aeronautical Univ. Daytona Beach, no. 171, (2014).
6. M. A. Mohammadi, A. Jafarian, "CFD simulation to investigate hydrodynamics of oscillating flow in a beta-type Stirling engine," *Energy*, vol. 153, (2018) pp. 287–300.
7. A. Ridha, A. Mohamed, C. Boualem, K. Tayeb, "Two-dimensional CFD simulation coupled with 6DOF solver for analyzing operating process of free piston stirling engine," *Journal of Advanced Research in Fluid Mechanics and Thermal Sciences*, vol. 55(1), (2019), pp. 29–38.
8. D. Gedeon, *Sage User's Guide*, Gedeon Associates, Athens, OH, Sage v11 Edition, (2016).
9. A. Abuelyamen, R. Ben-Mansour, H. Abualhamayel, E. M. A. Mokheimer, "Parametric study on beta-type Stirling engine," *Energy Conversion and Management*, vol. 145, (2017), pp. 53–63.
10. Z. Zhang and M. Ibrahim, "Development of CFD Model for Stirling Engine and its Components," *2nd International Energy Conversion Engineering Conference*, no. 37, (2004), pp. 1–11.
11. A. Sa Jalal, N. J. Baker, D. Wu, "Design of tubular moving magnet linear alternator for use with an external combustion - Free piston engine," *IET Conference Publications*, (2017).
12. J. R. Olson *et al.*, "Microcryocooler for tactical and space applications," *AIP Conference Proceedings*, vol. 1573, (2014), pp. 357–364.